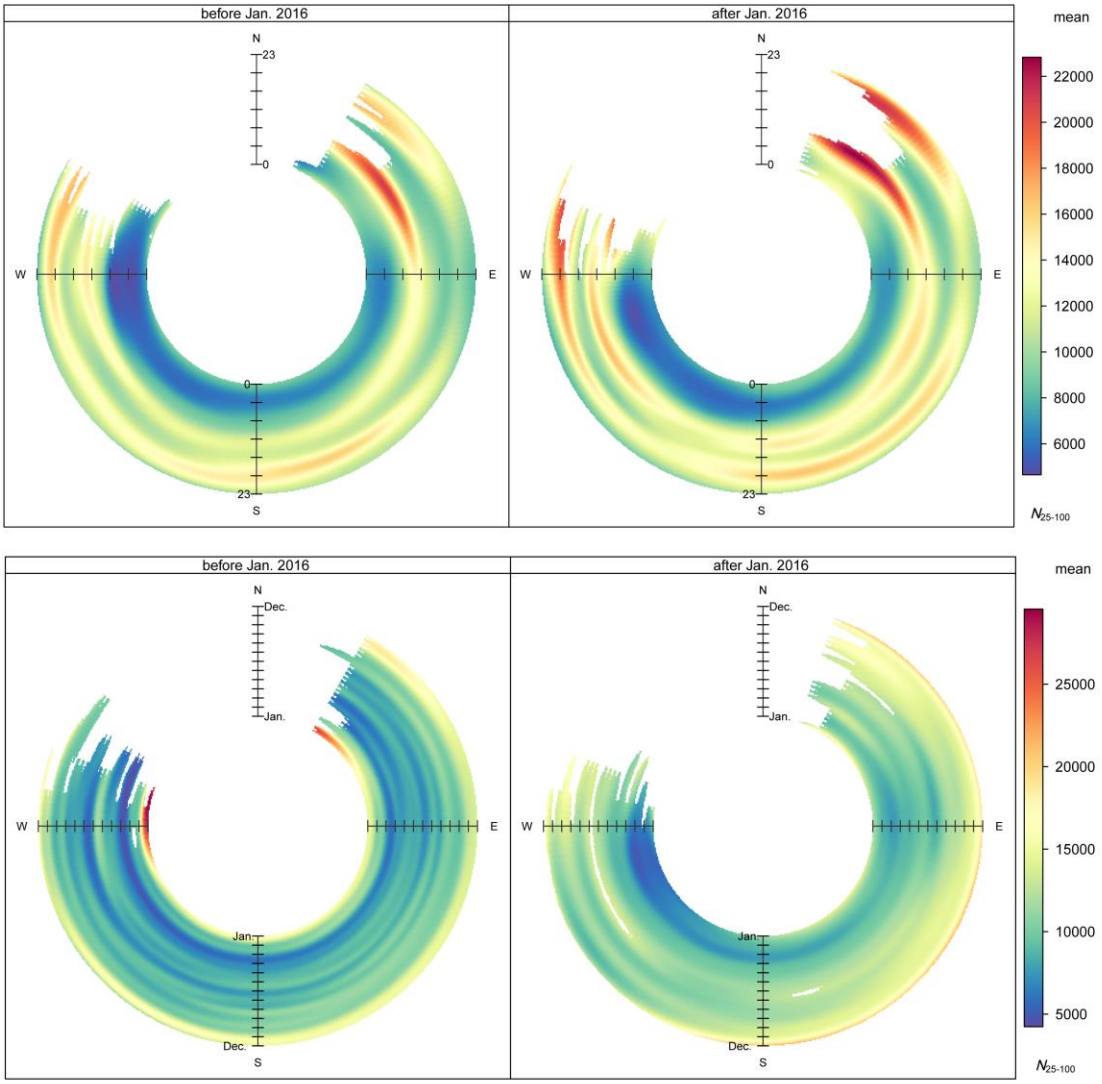

Figure S1: Mean diurnal (upper panel) and annual (lower panel) variations of particle number in 25-100 size bin ($N_{25\text{-}100}$) as wind directions before and after January 2016.

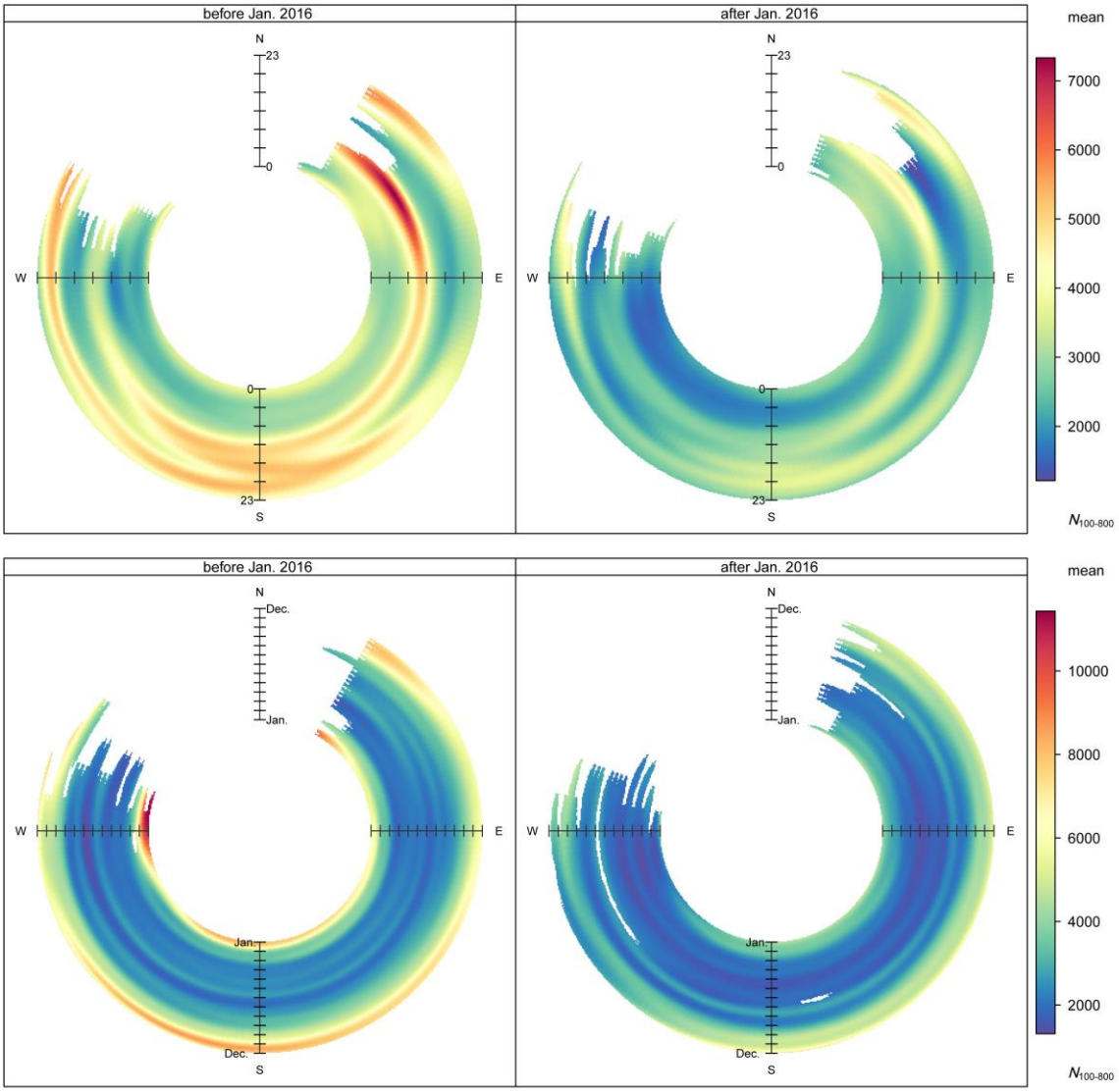

Figure S2: Mean diurnal (upper panel) and annual (lower panel) variations of particle number in 100-800 size bin ($N_{100\text{-}800}$) as wind directions before and after January 2016.

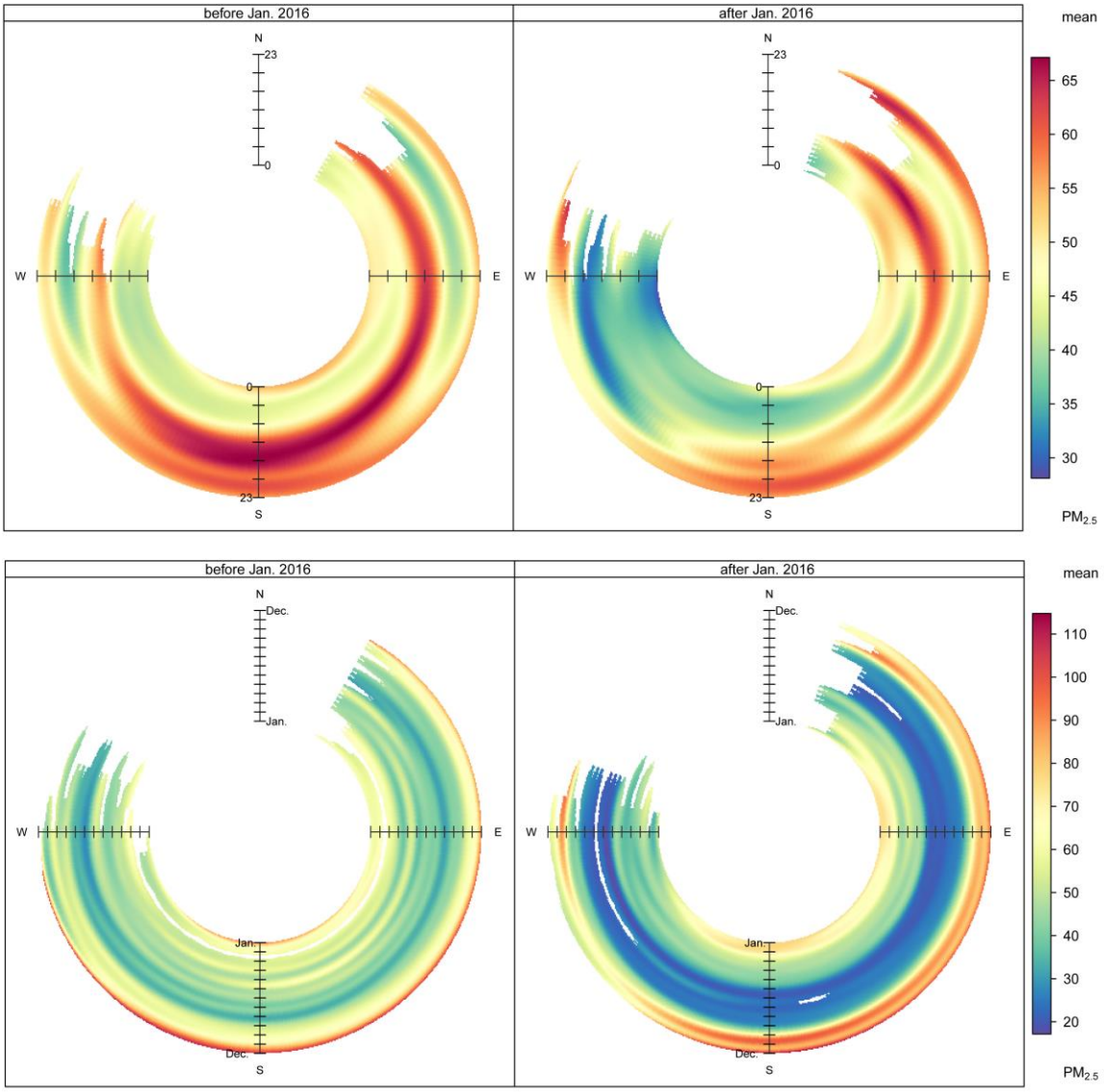

Figure S3: Mean diurnal (upper panel) and annual (lower panel) variations of $PM_{2.5}$ as wind directions before and after January 2016.

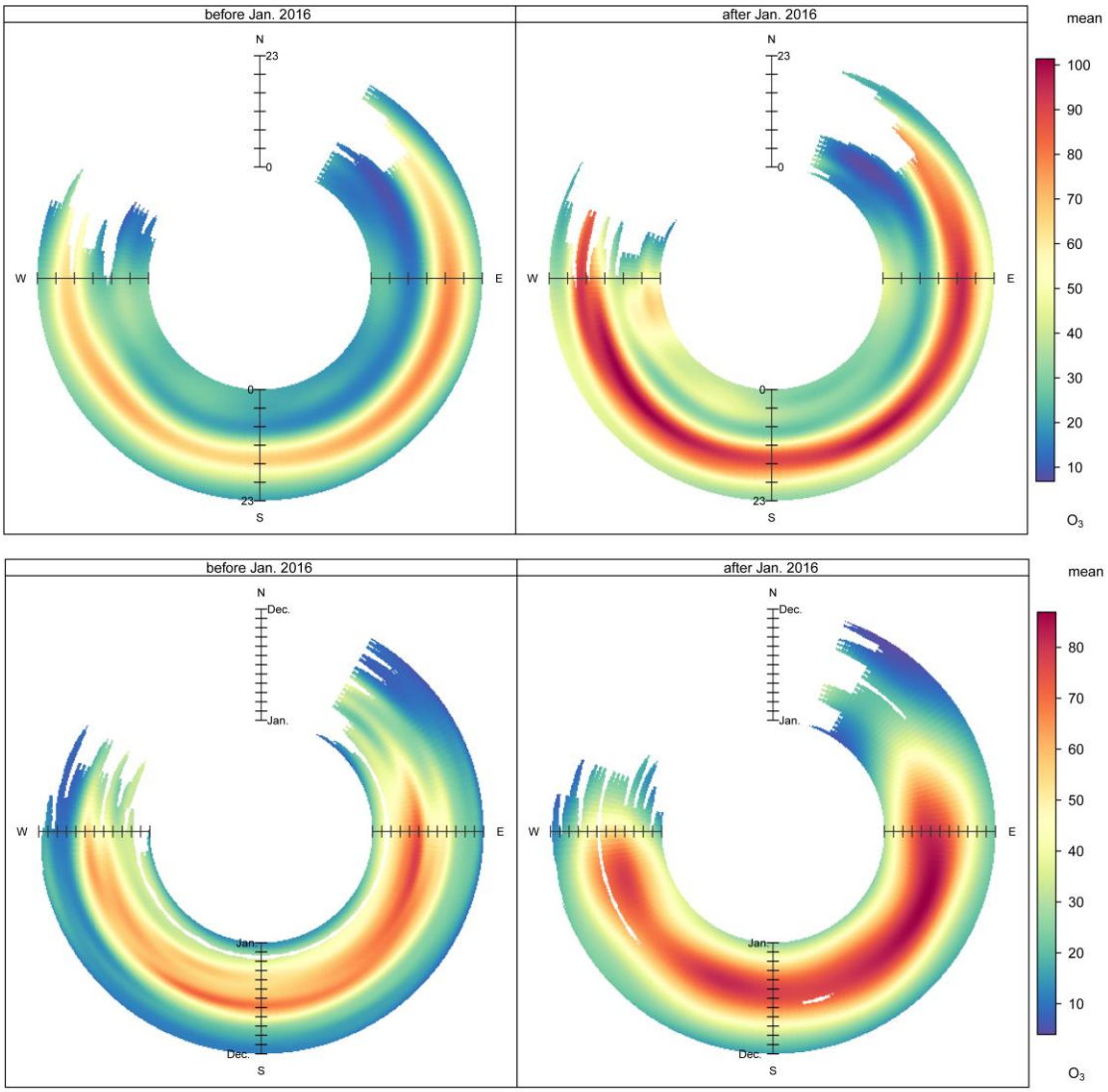

Figure S4: Mean diurnal (upper panel) and annual (lower panel) variations of O_3 as wind directions before and after January 2016.

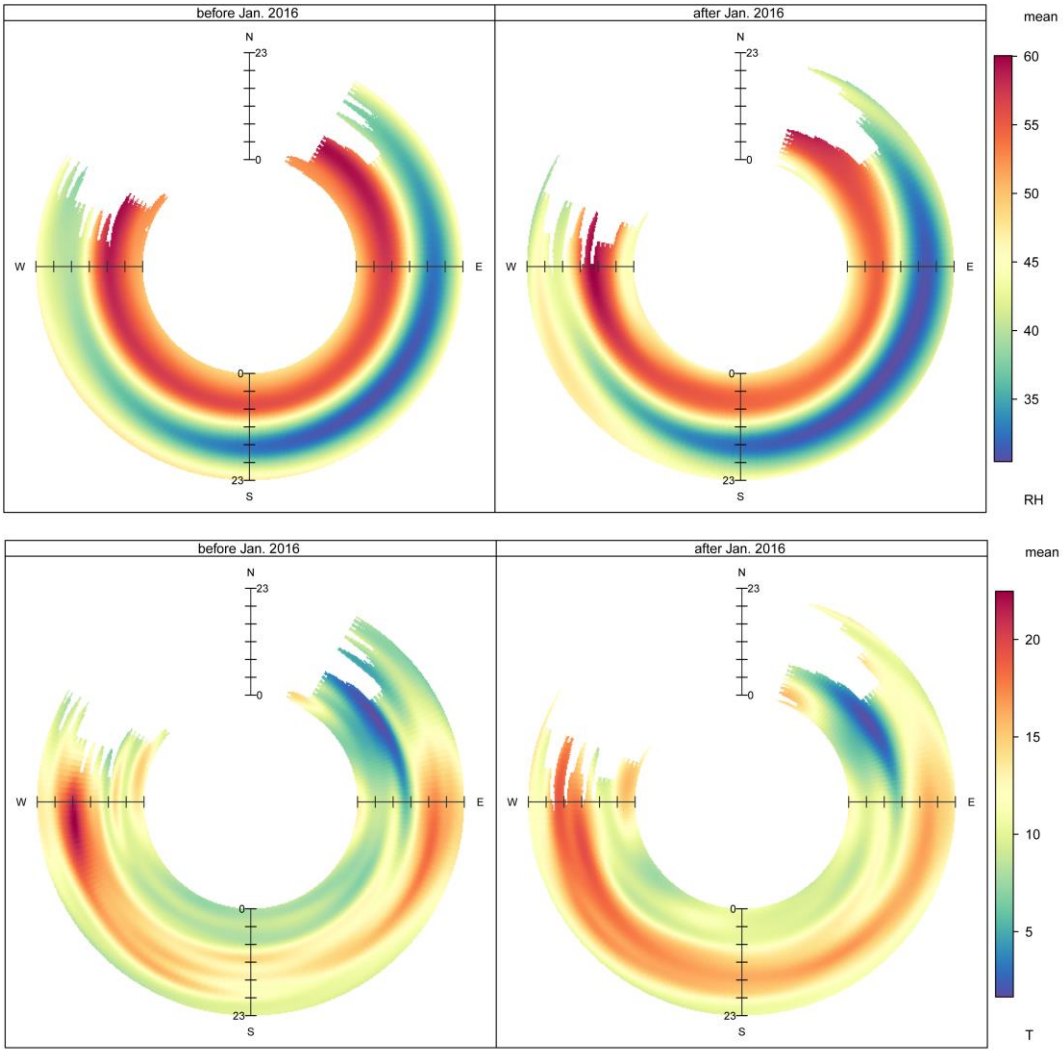

Figure S5: Mean diurnal variations of relative humidity (RH, upper panel) and temperature (T, lower panel) as wind directions before and after January 2016.

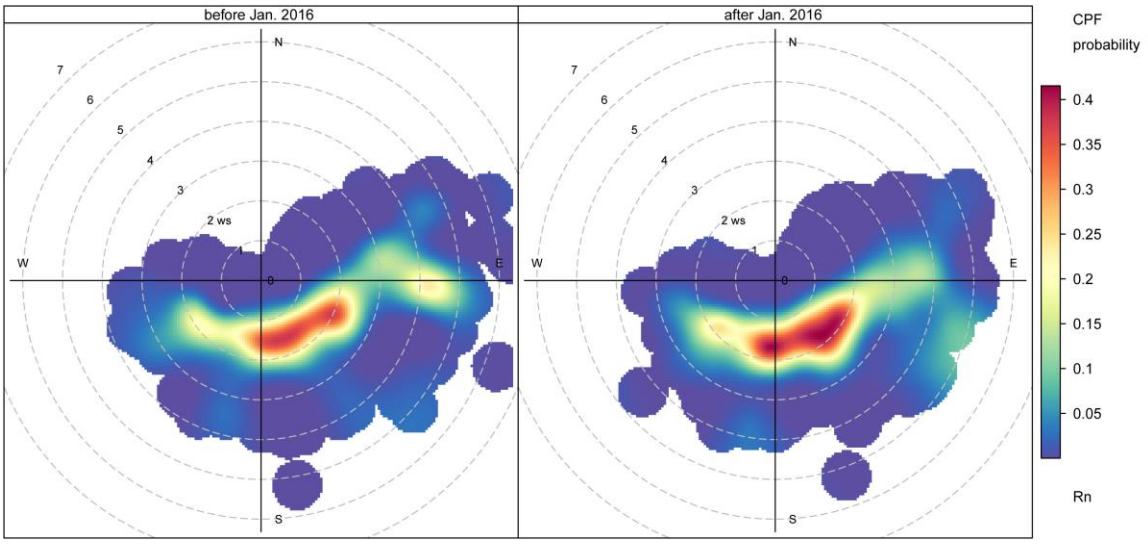

Figure S6: Polar plot of net radiation (Rn) based on the CPF function before and after January 2016.

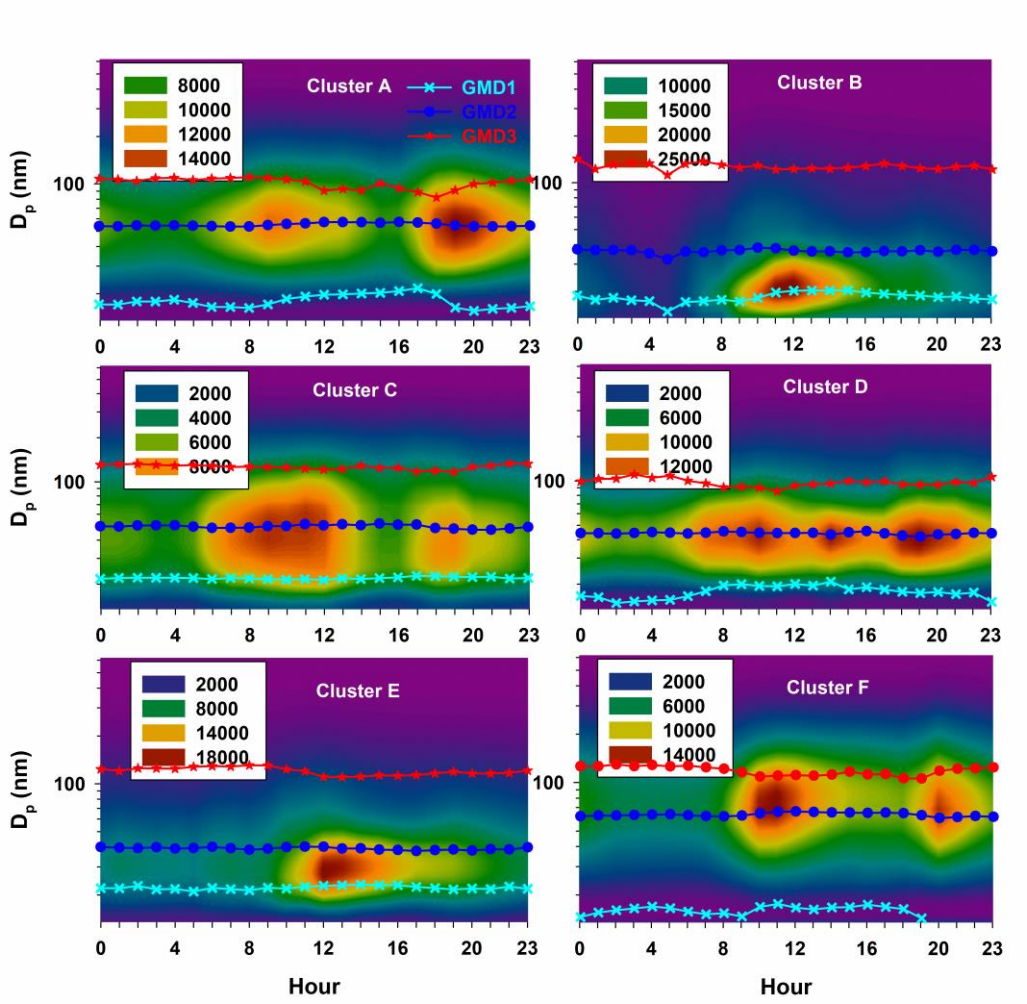

Figure S7: Averagely diurnal variations of particle number size distributions and geometric median diameter (GMD) of the three modes for Clusters A-F.

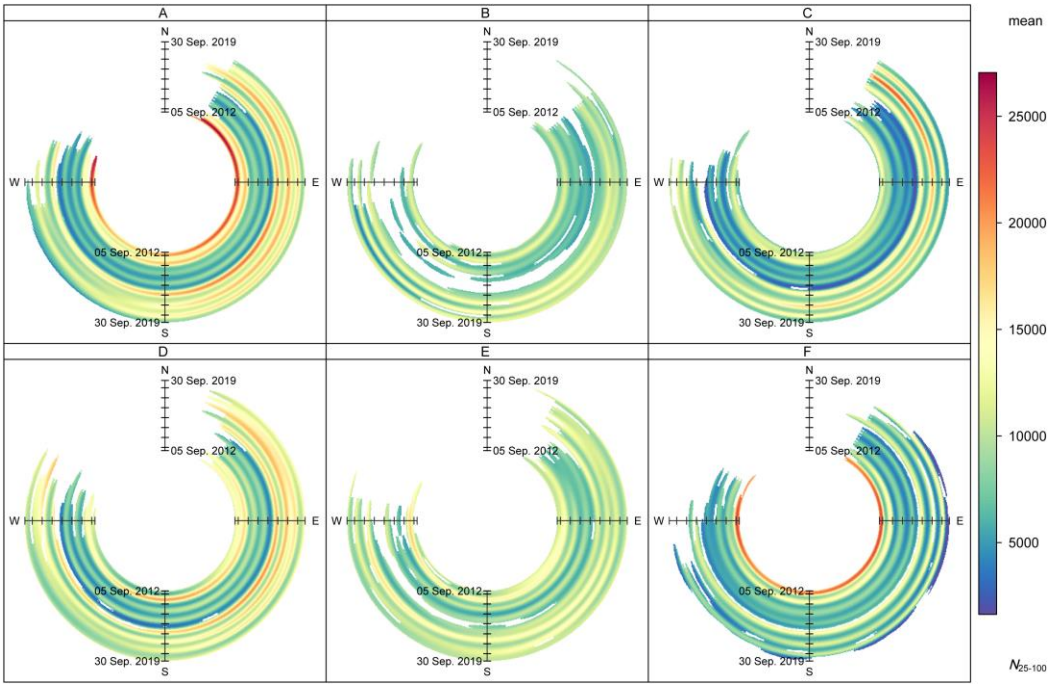

Figure S8: Trends of daily mean number of particles in Aitken mode ($N_{25\text{-}100}$) as wind directions for each cluster during the entire measurement campaign.

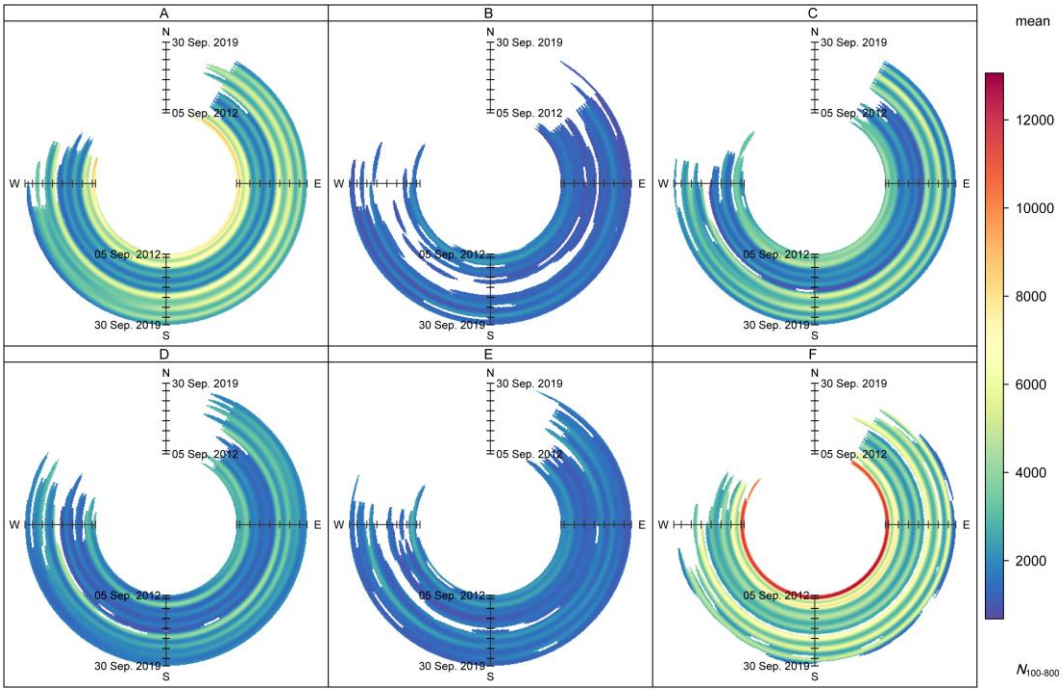

Figure S9: It is the same as Figure S8 but for accumulation mode ($N_{100\text{-}800}$).

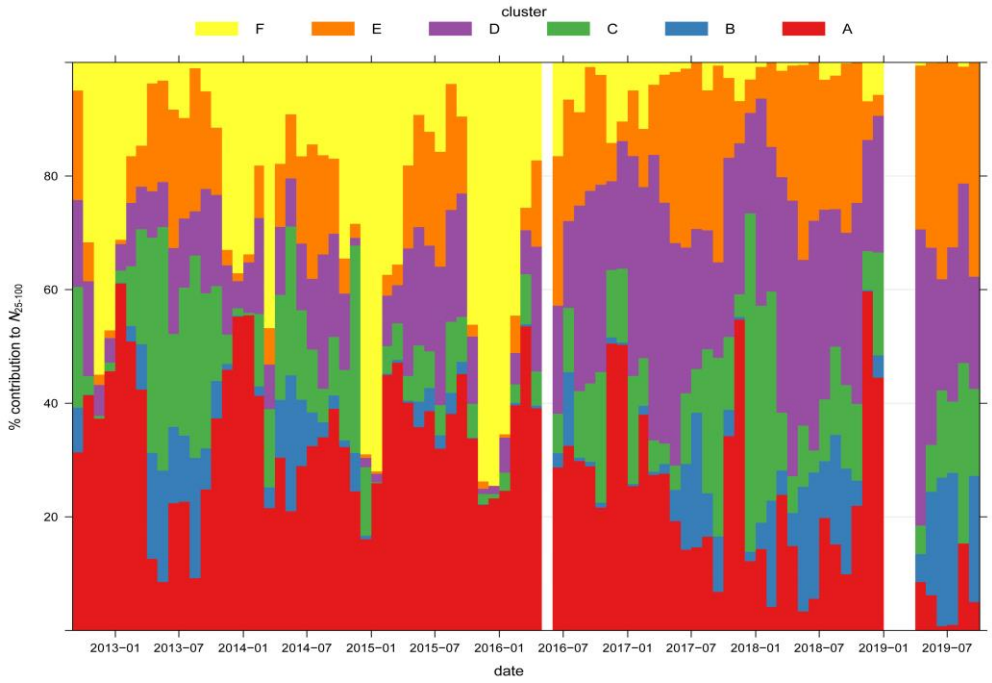

Figure S10: Variations of contribution of each cluster to monthly averaged $N_{25\text{-}100}$ during the entire measurement campaign.

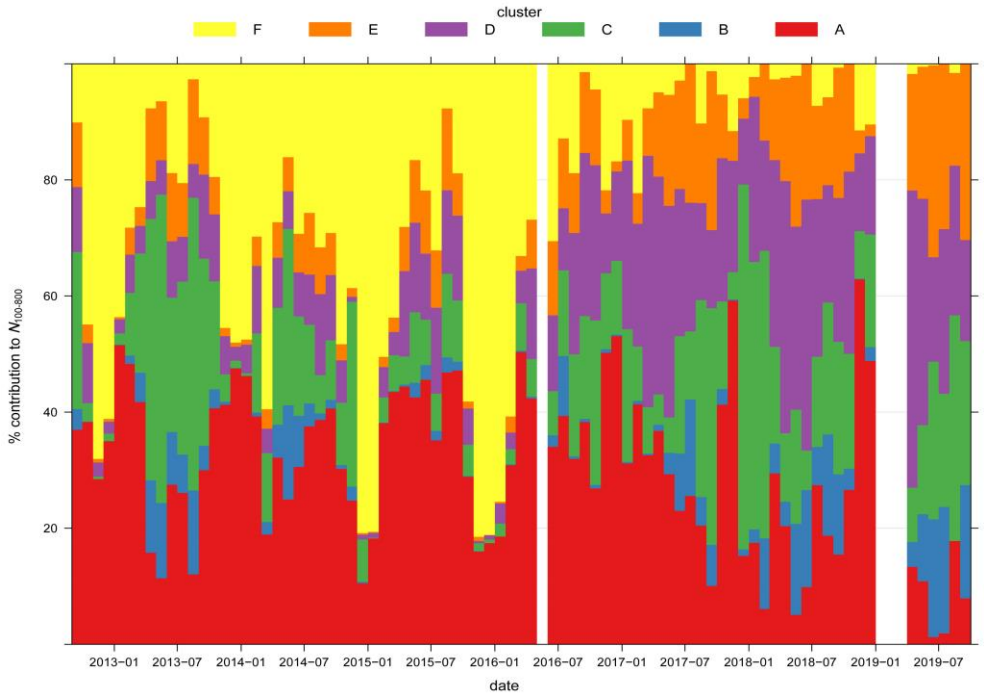

Figure S11: It is the same as Figure S10 but for monthly averaged $N_{100\text{-}800}$.

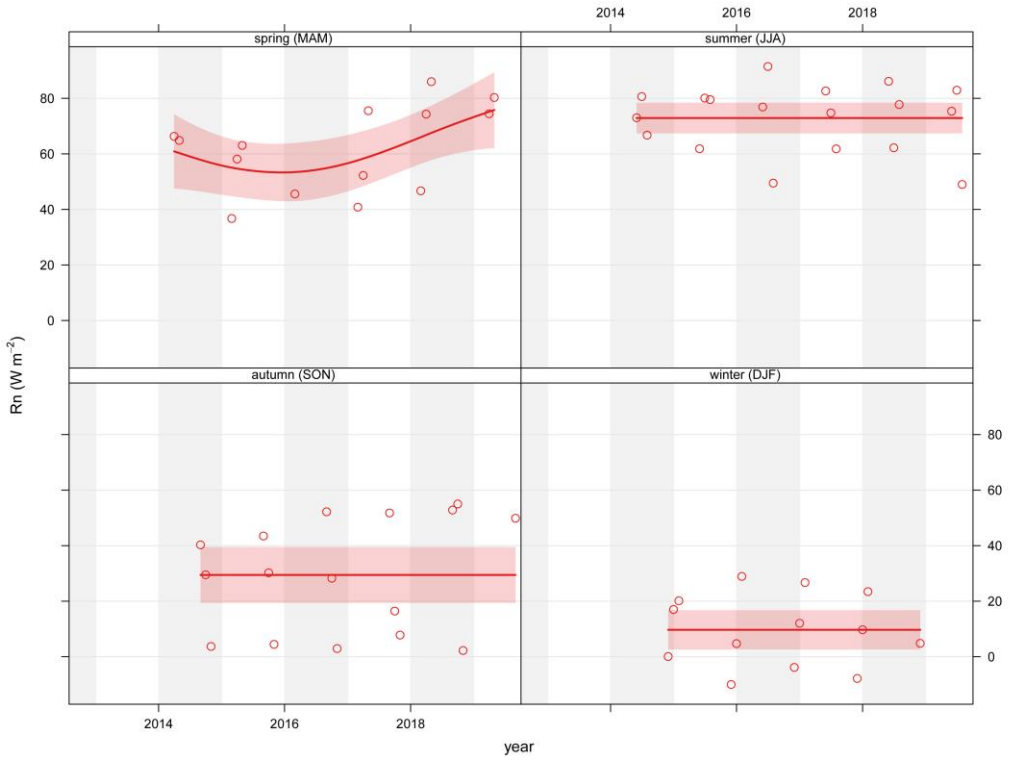

Figure S12: Inter-annual variations of monthly average Rn in four seasons. The monthly average concentrations are split by year and season. The smooth line is essentially determined using Generalized Additive Model, and the shading shows the estimated 95% confidence intervals.